General Disclaimer

- This document has been reproduced from the best copy furnished by the organizational source. It is being released in the interest of making available as much information as possible.

- This document may contain data, which exceeds the sheet parameters. It was furnished in this condition by the organizational source and is the best copy available.

- This document may contain tone-on-tone or color graphs, charts and/or pictures, which have been reproduced in black and white.

- This document is paginated as submitted by the original source.

- Portions of this document are not fully legible due to the historical nature of some of the material. However, it is the best reproduction available from the original submission.

RECOMPRESSION OF A TWO-DIMENSIONAL SUPERSONIC TURBULENT FREE SHEAR LAYER

by

Wen. L. Chow
Professor of Mechanical Engineering
Department of Mechanical and Industrial Engineering
University of Illinois at Urbana-Champaign
Urbana, Illinois 61801

ABSTRACT

A flow model has been devised to study the turbulent recompression process associated with a two-dimensional supersonic free shear layer. The flow field was divided into two subregions along the dividing streamline. The external supersonic free stream guides and interacts with the upper viscous layer. A velocity profile of third-degree polynomial was assumed for the upper viscous layer and the pressure difference across this layer was estimated from the normal momentum relationship. The lower viscous layer consisted of a forward flow with linear velocity profile and a back flow with a cosine profile. The difference in pressure across this layer was also accounted for. It was also pointed out that this analysis is equally applicable for cases with and without the downstream bounding wall. Conservation principles were subsequently applied to these regions and a system of ordinary differential and algebraic equations was obtained. In conjunction with the flow conditions prevailing at the end of the constant pressure jet mixing region, the system of equations may be integrated and solved numerically. For a given flow problem, the correct value of base pressure and the location along the wake boundary where recompression starts were established through iterations until the conditions at the rear stagnation point were satisfied. This procedure of calculations fully illustrated the typical elliptic behavior of all separated flow problems. Calculations for isoenergetic flow cases with thin initial boundary layers have been carried out and the results showed good agreement with the experimental data. It was also found from the results of calculations that the eddy diffusivity remained to be in the same order of magnitude as that of the constant pressure mixing region. With the suggested estimation for the eddy diffusivity within this recompression region, the turbulent normal stresses were also found to be one to two orders of magnitude smaller than the important flow quantities of such problems. These findings fully supported and justified the method of analysis suggested for this recompression process.

INTRODUCTION

For a flow passing a body with blunt trailing edge, the flow always separates away from the body ahead or at the base, creating a wake behind the body. The pressure within the wake, usually termed as the base pressure, is usually much lower than that of the free stream thus accounting for the large drag suffered by the body. This phenomenon exists irrespective of whether the problem is in the low speed or high speed flow regime. Since the advent of high speed flight, the base drag was recognized to be a serious problem, and a considerable amount of research has been directed into this area within the last two decades.

For a supersonic flow past a back step (see Fig. 1), it is recognized that the flow separates at the corner and the main flow will expand from the initial pressure to the lower base pressure. The initial boundary layer flow which is more or less guided by the free stream will also follow this expansion process. Along the early part of the wake boundary, the pressure is reasonably uniform, and for flows with large Reynolds number, a constant pressure turbulent jet mixing process occurs. Nearing the end of the wake, the main flow has to realign itself to the horizontal flow direction, initiating thereby a compressive process. As a result of this recompression, part of the fluid entrained within the viscous layer is turned back to form the recirculatory wake flow, while the rest will proceed downstream. Originally dealing with a simplified model for this flow problem, Korst [1] suggested an "escape criterion" associated with this recompression process. It specifies that the "dividing streamline" which separates the jet fluid from the wake fluid should assume such a mechanical energy level at the end of the jet mixing region that when it stagnates at the rear stagnation point through an isentropic (although irreversible-diabatic) process, its pressure is equal to the static pressure impressed behind the shock at the end of the wake. Employing this escape criterion would yield a unique base pressure solution for the problem. Experimental data have indicated, however, that the pressure at the rear stagnation point is much lower than what is impressed behind the shock. Nash [2], suggested empirical correlations of the two pressure levels. Page [3], Carriere and Sirieix [4], also developed empirical schemes individually to correlate characteristics associated with this recompression process.

Lees and his associates [5,6] considered this type of problem on an entirely different approach. Following the original idea suggested by Crocco and Lees [7], they treated the attached and separated viscous layers under one single framework, and showed that a critical point existed at the end of the wake (downstream of the rear stagnation point) which is somewhat similar to the nozzle throat. The correct base pressure associated with this type of flow assures a smooth flow passing through this critical point. Calculations for cases of turbulent flows have also been performed [8]. Extension to include the normal pressure gradient appeared recently [9]. Similar ideas were applied to laminar flow with axial-symmetric configurations by performing detailed numerical calculations for the outer flow [10]. However, the recompression flow process, particularly for turbulent flow, was never properly studied in detail. Other studies of wake flow problems are based on the method of integral relations [11], or complete numerical solutions of the Navier-Stokes equation [12]. These calculations require a considerable amount of time even with high speed computers and the turbulent flow cases have not been studied.

The present investigation was intended to consider this turbulent recompression process associated with a two-dimensional supersonic flow past a back step. A flow model which is equally applicable to laminar flows is presented. The establishment of the initial conditions for this recompression process is subsequently discussed. Numerical calculation procedures which illustrate the typical elliptic behavior of all separated flow problems are described. Finally, the results of calculations for flow cases with thin initial boundary layers and their comparison with the experimental data are presented and discussed.

Theoretical Flow Model

The present study of this recompression process is exclusively based on an integral approach. Referring to Fig. 2, the flow model guiding the present analysis can be described and discussed as follows:

1. The recompression region is split into two parts along the dividing streamline. The fluid above the dividing streamline will eventually proceed downstream, while the fluid below will be turned back to form the recirculatory wake flow as a result of recompression. The upper viscous layer interacts with the external inviscid stream; the latter guides and receives the influence of the former by following itself a Prandtl-Meyer compression relationship. This interaction is described by the fact that the transverse velocity component at the edge of the viscous layer induces an increase of pressure in the free stream which, in turn, influences the flow properties within the viscous layer, including this transverse velocity component at the edge of the viscous layer.

Integrating the continuity equation,

$$\frac{\partial(\rho u)}{\partial x} + \frac{\partial(\rho v)}{\partial y} = 0 \tag{1}$$

across the upper viscous layer, one obtains for the streamline angle at the edge of the viscous layer (see Fig. 3a)

$$\tan \beta_e = \frac{v_e}{u_e} = \frac{d}{dx}\left[\delta_a \int_0^1 \left(1 - \frac{\rho}{\rho_e}\phi\right) d\zeta\right]$$

$$- \frac{\delta_a \int_0^1 \frac{\rho}{\rho_e}\phi \, d\zeta}{(1 - c_e^2)^{1/(\gamma-1)} c_e} \frac{d}{dx}\left[(1 - c_e^2)^{1/(\gamma-1)} c_e\right] \tag{2}$$

where

$$\zeta = \frac{y}{\delta_a}, \quad \phi = \frac{u}{u_e}, \quad \text{and} \quad c_e = \frac{V_e}{V_{max}} = \frac{u_e}{V_{max}}$$

Since the free stream follows the Prandtl-Meyer relationship, the streamline angle β_e is related to the Prandtl-Meyer function ω by

$$\beta_e = \beta_\infty + \omega(c_\infty) - \omega(c_e) \tag{3}$$

where β_∞ is the difference of streamline angles between the dividing streamline and the free stream within the upstream constant pressure jet mixing region.

It is recognized, however, that the pressure difference across this upper viscous layer is not negligible. This difference can be calculated from

$$\frac{p_d}{p_e} = 1 + \frac{2\gamma}{\gamma - 1}\left\{\frac{c_e^2}{1 - c_e^2}\left(\tan^2 \beta_e - \tan \beta_e \frac{d\delta_a}{dx}\right) + \frac{1}{(1 - c_e^2)^{\gamma/(\gamma-1)}}\right.$$

$$\left. \cdot \frac{d}{dx}\left[(1 - c_e^2)^{1/(\gamma-1)} c_e^2 \left(\delta_a \int_0^1 \frac{\rho}{\rho_e}\phi^2 \tan \beta \, d\zeta - \frac{\varepsilon}{u_e}\int_{\phi_i}^1 \frac{\rho}{\rho_e} d\phi\right)\right]\right\} \tag{4}$$

with $\tan \beta = \tan \beta_e (2\zeta - \zeta^2)$, which is obtained by integrating the normal momentum equation,

$$\frac{\partial(\rho uv)}{\partial x} + \frac{\partial(\rho v^2)}{\partial y} = - \frac{\partial p}{\partial y} + \frac{\partial \tau_{xy}}{\partial x} \tag{5}$$

across the layer δ_a. The shear stress τ_{xy} in Eq. (5) has been evaluated by

$$\tau_{xy} = \rho \varepsilon \frac{\partial u}{\partial y}$$

where ε is the average eddy diffusivity across this layer and is, thus, a function of x only.†

2. For this upper viscous layer, a velocity profile of third-degree polynomials is assumed; namely,

$$\phi = \phi_d + \left.\frac{\partial \phi}{\partial \zeta}\right|_d \zeta + \left[3(1 - \phi_d) - 2 \left.\frac{\partial \phi}{\partial \zeta}\right|_d\right]\zeta^2 + \left[\left.\frac{\partial \phi}{\partial \zeta}\right|_d - 2(1 - \phi_d)\right]\zeta^3 \tag{6}$$

which obviously satisfies conditions of

$$\phi = \phi_d \ , \ \frac{\partial \phi}{\partial \zeta} = \left.\frac{\partial \phi}{\partial \zeta}\right|_d \text{ at } \zeta = 0 \ , \ \phi = 1 \ , \ \frac{\partial \phi}{\partial \zeta} = 0 \text{ at } \zeta = 1$$

In view of the fact that, at the rear stagnation point ($\phi_d = 0$), the shear stress at the dividing streamline should vanish, a simple correlation between the slope parameter $(\partial\phi/\partial\zeta)_d$ and ϕ_d would be that they shall be linearly proportional to each other; the constant of proportionality being determined from the initial condition prevailing at the end of the mixing region.

3. The lower viscous layer consists of a forward flow characterized by the dividing streamline velocity and a back flow characterized by a maximum back flow velocity. A linear velocity profile is assumed for the forward flow and a cosine profile for the back flow (see Fig. 3b). It was also recognized that the pressure difference across the lower viscous layer would influence the rate of recompression. For simplification purposes, it was assumed that the forward flow has the constant pressure p_d of the dividing streamline, while the back flow has the constant wall pressure p_w. The difference in pressure across this layer may be calculated from

$$\frac{p_w}{p_d} = 1 + \frac{1}{p_d}\left(\frac{dx}{dx_w} \sin \theta_\infty \tau_d - \frac{d}{dx_w}\int_0^{\delta_b} \rho u^2 \sin \theta_\infty \, dy\right) \tag{7}$$

which is the momentum relationship†† normal to x_w-direction for the small region as shown in Fig. 4a. If one further assumes that the dividing streamline and the line of zero-longitudinal velocity component follow straight line trajectories, Eq. (7) may be written for isoenergetic flows as

$$\frac{p_w}{p_d} = 1 + \frac{2\gamma}{\gamma - 1} \frac{\sin \theta_\infty}{(p_d/p_e)(p_e/p_{o\infty})} \left\{ \frac{\cos \theta_d}{\cos(\theta_\infty - \theta_d)} \frac{\tau_d}{\rho_\infty u_\infty^2} (1 - c_\infty^2)^{1/(\gamma-1)} c_\infty^2 \right.$$
$$\left. - \frac{d}{dx_w}\left[\frac{p_d}{p_e}\frac{p_e}{p_{o\infty}} \delta_b \left(\frac{1}{2c_d} \ln \frac{1 + c_d}{1 - c_d} - 1\right)\right]\right\} \tag{8}$$

---

†The expression for ε within such a recompression region is given later.

††Note that the contribution from the lateral shear stresses is small as the eddy

It should be mentioned that, for cases with the presence of the lower wall, one is compelled to consider the wall boundary layer of the back flow. It can be shown for the isoenergetic flow that, if the wall boundary layer has also a cosine flow profile, the total back flow mass and momentum fluxes would be the same as long as the back flow height and the maximum velocity are the same. The only difference between cases of with and without the wall is the wall shear stress, which is very small and can be neglected. Thus, flow cases of reattachment onto a solid wall are also included in the present formulation.

The geometry of the wake gives also relations such as

$$\frac{\delta_b}{\delta_{b\infty}} = \frac{\ell_{wk} - (\ell_m + x)}{\ell_{wk} - \ell_m} \tag{9}$$

$$\frac{\delta_b}{h_b} = \frac{\sin \theta_d}{\sin (\theta_\infty - \theta_d)} \tag{10}$$

where ℓ_{wk} is the length of the wake boundary. Application of the continuity principle across the lower viscous layer would produce a relationship which correlates the flow properties by (for isoenergetic flows)

$$\frac{\delta_b}{h_b} = \frac{4}{\pi} \frac{p_w}{p_d} \frac{c_d}{\sqrt{1 - c_b^2}} \tan^{-1} \frac{c_b}{\sqrt{1 - c_b^2}} \Bigg/ \left[-\ell n \, (1 - c_d^2)\right] \tag{11}$$

It should be noted that fluxes associated with the transverse velocity component (normal to the indicated velocity profiles) would not contribute significantly in the foregoing considerations because they are small in their order of magnitude; in addition, they tend to cancel each other.

4. Integral momentum principle is applied to both parts of the viscous layer (see Fig. 4) and two differential equations are obtained,

$$\frac{d}{dx}\left[\rho_e u_e^2 \delta_a \int_0^1 \frac{\rho}{\rho_e} \frac{u}{u_e}\left(1 - \frac{u}{u_e}\right) d\zeta\right] - \rho_e u_e \delta_a \int_0^1 \frac{\rho}{\rho_e} \frac{u}{u_e} d\zeta \frac{du_e}{dx} + p_e \frac{d\delta_a}{dx} - \frac{d}{dx}\left(p_e \delta_a \int_0^1 \frac{p}{p_e} d\zeta\right) = \tau_d \tag{12}$$

$$\frac{d}{dx}\left[p_d \delta_b + p_w h_b \cos \theta_\infty\right] + p_w \sin \theta_\infty \frac{dx_w}{dx} + \frac{d}{dx}\left[\rho_d u_d^2 \delta_b \int_0^1 \frac{\rho}{\rho_d}\left(\frac{u}{u_d}\right)^2 d\zeta + \rho_b u_b^2 h_b \int_0^1 \frac{\rho}{\rho_b}\left(\frac{u}{u_b}\right)^2 d\zeta \cos \theta_\infty\right] = \tau_d \tag{13}$$

Upon introducing

$$\frac{p}{p_e} = \frac{p_d}{p_e} - \frac{3}{2}\left(\frac{p_d}{p_e} - 1\right)\zeta + \frac{1}{2}\left(\frac{p_d}{p_e} - 1\right)\zeta^3$$

into Eq. (12) for the pressure variation across the upper layer, and the assumed profiles for the lower viscous layer into Eq. (13) and normalizing, Eqs. (12) and (13) become, for isoenergetic flows,

$$\frac{d}{dx}\left[(1 - c_e^2)^{1/(\gamma-1)} c_e^2 \delta_a \int_0^1 \frac{\rho}{\rho_e}\phi(1 - \phi)\, d\zeta\right] + (1 - c_e^2)^{1/(\gamma-1)} c_e \delta_a \cdot \int_0^1 \left(1 - \frac{\rho}{\rho_e}\phi\right) d\zeta \frac{dc_e}{dx} - \frac{3}{16}\frac{\gamma - 1}{\gamma}\frac{d}{dx}\left[(1 - c_e^2)^{\gamma/(\gamma-1)}\delta_a\left(\frac{p_d}{p_e} - 1\right)\right] = \frac{\tau_d}{\rho_\infty u_\infty^2}(1 - c_\infty^2)^{1/(\gamma-1)} c_\infty^2 \tag{12a}$$

and

$$-\frac{\gamma - 1}{2\gamma}\frac{d}{dx}\left[\frac{p_d}{p_e}\frac{p_e}{p_{o\infty}}\left(\delta_b + \frac{p_w}{p_d} h_b \cos\theta_\infty\right)\right] + \frac{\gamma - 1}{2\gamma}\sin\theta_\infty \frac{\cos(\theta_\infty - \theta_d)}{\cos\theta_d} \cdot \frac{p_w}{p_d}\frac{p_d}{p_e}\frac{p_e}{p_{o\infty}} + \frac{d}{dx}\left\{\frac{p_d}{p_e}\frac{p_e}{p_{o\infty}}\left[\delta_b\left(\frac{1}{2c_d}\ln\frac{1 + c_d}{1 - c_d} - 1\right) + \frac{p_w}{p_d} h_b \cos\theta_\infty \cdot \left(\frac{1}{\sqrt{1 - c_b^2}} - 1\right)\right]\right\} = \frac{\tau_d}{\rho_\infty u_\infty^2}(1 - c_\infty^2)^{1/(\gamma-1)} c_\infty^2 \tag{13a}$$

The shear stress τ_d which appears at the right sides of these two equations is evaluated from an eddy diffusivity formulation for this recompression process which assumes the same form as that of the preceding constant pressure mixing region and the equivalent σ value is assumed to vary inversely as the upper viscous layer thickness; namely

$$\varepsilon = \frac{1}{4\sigma^2}(\ell_m + x)\, u_e \quad \text{with} \quad \frac{\sigma}{\sigma_\infty} = \frac{\delta_{a\infty}}{\delta_a}$$

Thus, the shear stress term appearing in both Eqs. (12a) and (13a) can be evaluated from

$$\frac{\tau_d}{\rho_\infty u_\infty^2}(1 - c_\infty^2)^{1/\gamma - 1}\, c_\infty^2 = \frac{\varepsilon}{u_e \delta_a}\frac{\rho}{\rho_e}\bigg|_d \frac{\partial\phi}{\partial\zeta}\bigg|_d (1 - c_e^2)^{1/\gamma - 1} c_e^2 \tag{14}$$

5. The initial conditions are provided for from the upstream constant pressure jet mixing process. In order to achieve a smooth joining between the mixing and recompression regions, a constant pressure turbulent jet mixing analysis was performed by adopting a velocity profile compatible with that for the recompression study.

Fully Developed Constant Pressure Turbulent Jet Mixing

Upon employing the momentum principle

$$\frac{d}{dx}\int_{-\delta_b}^{0} \rho u^2\, dy = \tau_d = \frac{d}{dx}\int_0^{\delta_a} \rho u(u_\infty - u)\, dy$$

and the stipulation that the velocity profile slope at the dividing streamline matches with that of an error function profile, *i.e.*,

$$\frac{d\phi}{d\eta}\bigg|_d = \frac{1}{\sqrt{\pi}}$$

It may be shown that, for such an isoenergetic fully developed jet mixing region, all flow quantities are functions of a dimensionless homogeneous coordinate $\eta[\eta = \sigma_\infty(y/x)]$ only and following relations are obtained

$$\frac{c_\infty^3}{4\pi} = (1 - c_{d\infty}^2)\left(\frac{1}{2}\ln\frac{1 + c_{d\infty}}{1 - c_{d\infty}} - c_{d\infty}\right) \tag{15}$$

$$\left.\frac{d\phi}{d\zeta}\right|_d = \frac{\eta_a}{\sqrt{\pi}} \tag{16}$$

$$\eta_b = \phi_{d\infty}\sqrt{\pi} \tag{17}$$

and

$$\frac{1}{4\sqrt{\pi}}\frac{1 - c_\infty^2}{1 - c_{d\infty}^2} = \eta_a\int_0^1 \frac{\rho}{\rho_\infty}\phi(1 - \phi)\,d\zeta \tag{18}$$

where

$$\phi = \phi_{d\infty} + \left.\frac{d\phi}{d\zeta}\right|_{d\infty}\zeta + \left[3(1 - \phi_{d\infty}) - 2\left.\frac{d\phi}{d\zeta}\right|_{d\infty}\right]\zeta^2 + \left[\left.\frac{d\phi}{d\zeta}\right|_{d\infty} - 2(1 - \phi_{d\infty})\right]\zeta^3 \left(\text{for } \zeta > 0,\ \phi = \frac{u}{u_\infty},\ \zeta = \frac{y}{\delta_{a\infty}}\right)$$

and

$$\phi = (1 + \zeta)\left(\text{for } -1 < \zeta < 0,\ \zeta = \frac{y}{\delta_{b\infty}},\ \phi = \frac{u}{u_{d\infty}}\right)$$

have been used as the velocity profile. Values of $\eta_a = \sigma_\infty\delta_{a\infty}/\ell_m$ and $\eta_b = \sigma_\infty\delta_{b\infty}/\ell_m$ are solved from these relations.

Developing Flows

For all practical flow cases, the flow at the end of the mixing region is never fully developed and the initial boundary layer has predominant influence on the recompression process. For thin initial boundary layers,† it was shown by Hill and Page, Carriere and Sirieix, and Korst and Chow that the effect of its presence may be accounted for through the origin shift concept [13] and the equivalent bleed concept [4,14]. Thus, the initial flow properties of the recompression region can be obtained from the corrections of the fully developed flow through

$$\delta_{a\infty} = \eta_a(\ell_m + x_o)/\sigma_\infty \tag{19}$$

$$\delta_{b\infty} = \eta_b(\ell_m + x_o)/\sigma_\infty \tag{20}$$

where

$$x_o = \frac{\sigma\theta_2}{\int_{-\eta_b}^{\eta_a}\frac{\rho}{\rho_\infty}\frac{u}{u_\infty}\left(1 - \frac{u}{u_\infty}\right)d\eta\Big|_{fd}} \tag{21}$$††

is the origin shift, θ_2 being the momentum thickness of the profile at the beginning of the mixing region. The dividing streamline velocity ($c_{d_{nfd}}$) for the non-fully developed flow is found from

$$[-\ln(1 - c_{d_{nfd}}^2)] = \frac{2c_{d\infty}^2}{(1 - c_\infty^2)\phi_{d\infty}\eta_b}\left[\int_{-\eta_b}^{\eta_a}\frac{\rho}{\rho_\infty}\frac{u}{u_\infty}\left(1 - \frac{u}{u_\infty}\right)d\eta\Big|_{fd} - \frac{\sigma_\infty\theta_2}{\ell_m}\right] \tag{22}$$

The streamline angle β_∞ appearing in Eqs. (3) can be approximately estimated by

---

†The effect of lip shock is also disregarded. Thus, the present calculation is also restricted to low supersonic free stream Mach numbers.

††Henceforth, fd denotes fully developed, while nfd denotes non-fully developed

$$\tan \beta_\infty = \frac{\eta_s}{\sigma_\infty} \int_0^1 \left(1 - \frac{\rho}{\rho_\infty} \phi\right) d\zeta \Big|_{s f d} \tag{23}$$

and the relationship concerning the spread rate parameter

$$\sigma_\infty = 12 + 2.76 M_\infty$$

has been tacitly employed [13].

It should be emphasized that these correction techniques are valid only for thin approaching initial boundary layers.

CALCULATION PROCEDURES

Specializing for isoenergetic flows, one may select for given initial conditions a pair of values for the base pressure ratio p_b/p_1 and the length ℓ_m† along the wake where recompression starts. The momentum thickness of the viscous layer at the beginning of jet mixing may be calculated by White's formula [15]

$$\frac{\theta_2}{\theta_1} = \left(\frac{c_1}{c_\infty}\right)^{3.2} \left(\frac{1 - c_1^2}{1 - c_\infty^2}\right)^{1.4} \tag{24}$$

or the streamtube expansion method and the initial conditions required for recompression study may be established according to the previously described scheme. One may start to integrate the system of differential equations through a step-by-step procedure. At each location along the course of recompression, the free stream Crocco number c_e and the dimensionless dividing streamline velocity ϕ_d may be selected and iterated upon until the system of equations is satisfied. It may be noted that, for each pair of values of c_e and ϕ_d, δ_s may be found from Eq. (2), p_d/p_e from Eq. (4), δ_b from Eq. (9), p_w/p_d from Eq. (8), h_b from Eq. (10), and c_b from Eq. (11). Upon substituting all this information into Eqs. (12a) and (13a), two residues are usually obtained. Values of c_e and ϕ_d at this location should be iterated upon until these residues vanish.

These calculations can be continued until the rear stagnation point is reached. At this location, ϕ_d is set to zero and the wall pressure becomes the stagnation pressures of both the dividing streamline and the representative back flow. From the normal momentum relationship given by Eq. (8), the correct free stream Crocco number at the stagnation point can be established when the wall pressure is obtained from the intersection (and averaging) of previously established curves for p_{od} and p_{ob}. Again, two residues are usually obtained from Eqs. (12a) and (13a) at the rear stagnation point.

The initially selected values of the base pressure ratio p_b/p_1 and the location ℓ_m where recompression starts have to be iterated upon until the residues of the system of equations at the rear stagnation point are reduced to zero. The correct flow field is thus established up to the rear stagnation point.

It is worthwhile to point out that this scheme of calculations and iterations exhibits the typical elliptic behavior of all separated flow problems. The fact that the value of the base pressure ratio is uniquely determined according to the conditions associated with the rear stagnation point is well evidenced by the method of calculation of this recompression process up to the rear stagnation point. In addition, the correct flow pattern established at the point of reattachment serves also as the initial condition for the downstream flow field where additional recompression and flow rehabilitation occur.

---

†Note that, for numerical calculations, all lengths have been normalized by the step height H.

RESULTS OF CALCULATIONS†

Figure 5 shows the pressure distribution on the wall for the flow case of $M_1 = 2.0$, $\theta_1/H = 0.014$. The base pressure ratio p_b/p_1 determined from these calculations is 0.362. It can be seen that the calculated pressure distribution up to the point of reattachment showed excellent agreement with the experimental data which were obtained in the blow down facilities at the University of Illinois. Figure 6 shows also results indicating variations of p_{od}, p_{ob}, ϕ_b, and $\phi_b(\phi_b = u_b/u_e)$. It is particularly interesting to see that the dividing streamline is being energized continuously throughout this part of the recompression process.

Figure 7 shows another calculation for $M_1 = 2.25$, $\theta_1/H = 0.01$. Again, the base pressure agreed well with the experimental data.

Figure 8 shows the variation of base pressure with respect to the initial momentum thickness of the boundary layer at $M_1 = 2.0$. It also shows that the theoretical results presented by Alber and Lees [8] are too high, especially for cases with thin initial boundary layers. Pertinent experimental data from elsewhere are also included in the same figure.

Figure 9 presents results of calculations for $M_1 = 1.56$ as functions of the initial momentum thickness. Results for one set of flow conditions of $M_1 = 3.0$, $\theta_1/H = 0.003$ have also been obtained. The base pressure of $p_b/p_1 = 0.133$ agrees very well with the experimental data compiled by Reda and Page [6] and reproduced in Fig. 10.

It should be pointed out that, in all these calculations, the influence of the pressure variations across the upper viscous layer to the density was not accounted for and the density was estimated as if the viscous layer had the constant free stream pressure; *i.e.*,

$$\rho/\rho_e = (1 - c_e^2)/(1 - c_e^2\phi^2)$$

Also, in estimating the pressure difference across the layer, the shear stress term has been ignored in Eq. (8).

DISCUSSION AND CONCLUSIONS

In comparing theoretical calculations with the experimental data, it appears that the method suggested here for the reattachment process produced reasonable results. In view of the lack of knowledge in the eddy diffusivity within the recompression region and the inadequate data concerning the spread rate of the preceding constant pressure mixing process, it is felt that the analysis suggested here can only be considered as a workable scheme. In addition, there is considerable room for improvement to the present analysis. Particularly for cases of thick initial boundary layers, the upstream jet mixing as well as the recompression region may well have been imbedded within a rotational flow field and a "local freestream" concept would seem to be useful under these situations.

Nevertheless, it is interesting to point out that, under the present formulation of the eddy diffusivity, the normal turbulent stresses have been found to be one to two orders of magnitude smaller than the important flow quantities. In addition, the eddy diffusivity was found to remain in the same order of magnitude as that of the preceding constant pressure mixing region. These findings fully support and justify the method of analysis suggested for such a recompression process.

Further calculations toward downstream direction are possible by adopting the

---

†All calculations were carried out on a digital computer IBM 7094, Department of Physics, University of Illinois at Urbana-Champaign.

same system of equations. Referring to Fig. 11 where the initial conditions for downstream calculations can be estimated from the information obtained at the rear stagnation point, it may be anticipated that the characteristic feature of the flow is the realignment of the external inviscid stream into the original horizontal flow direction and it is believed that any shear stress acting along the centerline may be again ignored. From Eqs. (2) and (12a), it may be observed that relaxation of the pressure difference across the viscous layer provides the main balancing factor, at least in the early part of the flow rehabilitation. The final equilibrium state is reached only when the main flow is in the horizontal direction.

Finally, it is worthwhile to point out that the suggested flow model may be employed to study flow problems in many other flow regimes. Upon combining with the conformal mapping technique, it is hoped that many of the incompressible flow problems may be studied.

ACKNOWEDGMENTS

This work is partially supported by NASA through Research Grant NGL 14-005-140 entitled "Fluid Dynamic and Heat Transfer Problems Associated with Modern Propulsive Systems." This problem was initiated during the summer of 1969 while the author was a summer consultant with RTF, ARO, Inc., Tullahoma, Tennessee. Acknowledgment is due to Mr. F. Minger for his interest and encouragement, Messers C. E. Peters, R. C. Bauer, and C. E. Willbanks for their interesting discussions. The author is also indebted to Professor R. A. White and Mr. P. Gerhart for providing the experimental data obtained at the University of Illinois.

REFERENCES

1. Korst, H. H., "A Theory for Base Pressures in Transonic and Supersonic Flow," Journal of Applied Mechanics, Vol. 23, 1956, pp. 593-600.

2. Nash, J. F., "An Analysis of Two-Dimensional Turbulent Base Flow Including the Effect of the Approaching Boundary Layer," NPL Aero Report No. 1036, 1962.

3. Page, R. H., Hill, W. G., Jr., and Kessler, T. J., "Reattachment of Two-Dimensional Supersonic Turbulent Flows," ASME Paper 67-F-20, presented at the Fluids Engineering Conference, Chicago, Illinois, May 8-11, 1967.

4. Carriere, P., and Sirieix, M., "Résultats Récents dans l'Etude des Problèmes de Mélange et de Recollement," XI Congres Internal de Mecaniquee, Munich, T. P. 165 (1964) ONERA, September 1964.

5. Lees, L., and Reeves, B. L., "Supersonic Separated and Reattaching Laminar Flows: 1. General Theory and Application to Adiabatic Boundary Layer/Shock Wave Interactions," AIAA Journal, Vol. 2, 1964, pp. 1907-1920.

6. Reeves, B. L., and Lees, L., "Theory of the Laminar Near Wake of Blunt Bodies in Hypersonic Flow," AIAA Journal, No. 3, 1965, pp. 2061-2074.

7. Crocco, L., and Lees, L., "A Mixing Theory for the Interaction between Dissipative Flows and Nearly Isentropic Streams," Journal of Aerospace Science, Vol. 19, 1952, pp. 649-676.

8. Alber, I. E., and Lees, L., "Integral Theory for Supersonic Turbulent Base Flows," AIAA Journal, Vol. 6, 1968, pp. 1343-1351.

9. Shammoth, S. J., and McDonald, H., "A New Solution of the Near Wake Recompression Problem," paper presented at AIAA Eighth Aerospace Sciences Meeting, December 1969.

10. Ohrenberger, J. T., and Baum, E., "A Theoretical Model of the Near Wake of a Slender Body in Supersonic Flow," AIAA paper No. 70-792, presented in AIAA

11. Nielsen, J. N., Lynes, L. L., and Goodwin, F. K., "Calculation of Laminar Separation with Free Interaction by the Method of Integral Relations," Report AFFDL-TR-65-107, Part II, VIDYA Division, ITEK Corporation, January 1966.

12. Roache, P. J., and Mueller, T. J., "Numerical Solutions of Laminar Separated Flows," AIAA Journal, Vol. 8, 1970, pp. 530-538.

13. Hill, W. G., Jr., and Page, R. H., "Initial Development of Turbulent, Compressible Free Shear Layers," Journal of Basic Engineering, Vol. 91, 1969, pp. 67-73.

14. Korst, H. H., and Chow, W. L., "Non-Isoenergetic Turbulent Jet Mixing between Two Compressible Streams at Constant Pressure," NASA CR-419, 1965.

15. White, R. A., "Effect of Sudden Expansions or Compressions on the Turbulent Boundary Layer," AIAA Journal, Vol. 4, 1966, pp. 2232-2234.

16. Reda, D. C., and Page, R. H., "Supersonic Turbulent Flow Reattachment Downstream of a Two-Dimensional Backstep," Report AFOSR 69-1592 TR or RU-TR 125-MAE-F, Department of Mechanical and Aerospace Engineering, Rutgers University, New Brunswick, New Jersey, May 1969.

NOMENCLATURE

c	V/V_{max}, Crocco number
c_b	Crocco number for back flow of maximum velocity
H	step height
h_b	height for back flow
ℓ_m	length of the constant pressure region along the wake boundary, measured from separation corner
ℓ_{wk}	$H/\sin\theta_\infty$, length of the wake boundary measured from the separation corner to the point of reattachment
M	Mach number
p	pressure
u	x-velocity component
V	magnitude of velocity
v	y-velocity component
x	coordinate in main flow direction
y	coordinate normal to x
ρ	density
β	streamline angle
δ	thickness of viscous layer
ϕ	u/u_e, dimensionless velocity
ζ	y/δ_a or y/δ_b
$\omega(c)$	$\sqrt{(\gamma+1)/(\gamma-1)}\,\tan^{-1}\sqrt{[(c^2-(\gamma-1)/(\gamma+1)]/[1-c^2)} - \tan^{-1}\sqrt{\dfrac{[(\gamma+1)/(\gamma-1)\,c^2-1]}{1-c^2}}$,
γ	ratio of specific heat
τ	shear stress
ε	eddy diffusivity
θ	angle or momentum thickness
η	$\sigma y/x$
σ_∞	similar parameters for constant pressure jet mixing regions

Subscripts

a	viscous layer above the dividing streamline
b	viscous layer below the dividing streamline or back flow
d	dividing streamline
e	external inviscid stream
w	wall or centerline state
0	stagnation state
1	approaching flow state
2	flow state after the Prandtl-Meyer expansion
∞	station at the beginning of recompression

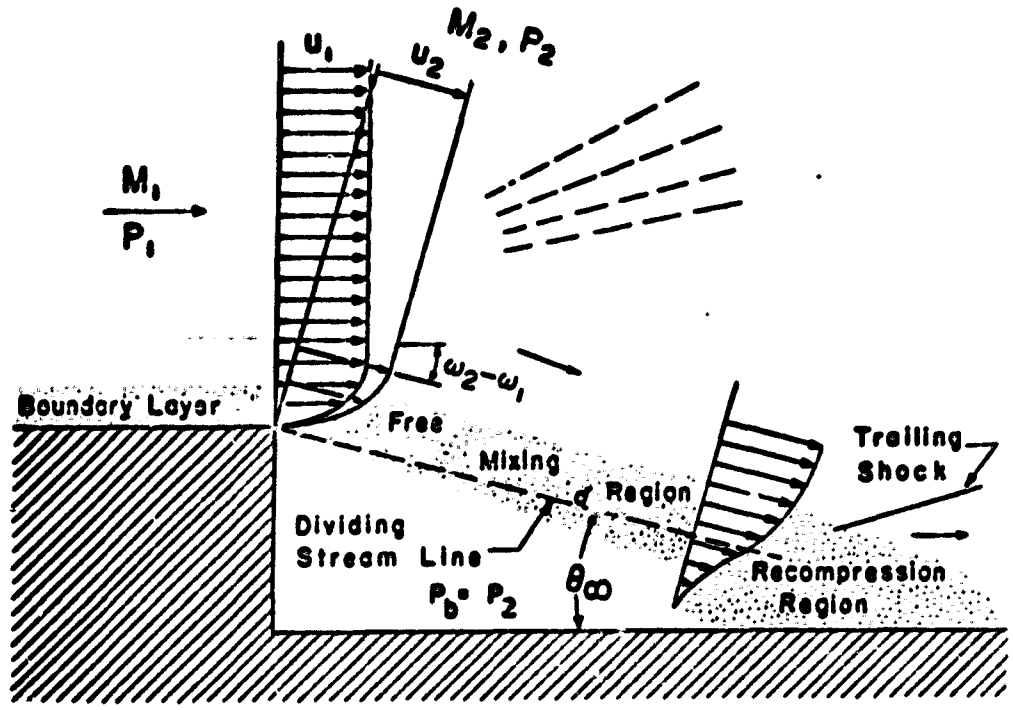

Figure 1 Two-Dimensional Supersonic Flow Past a Back Step

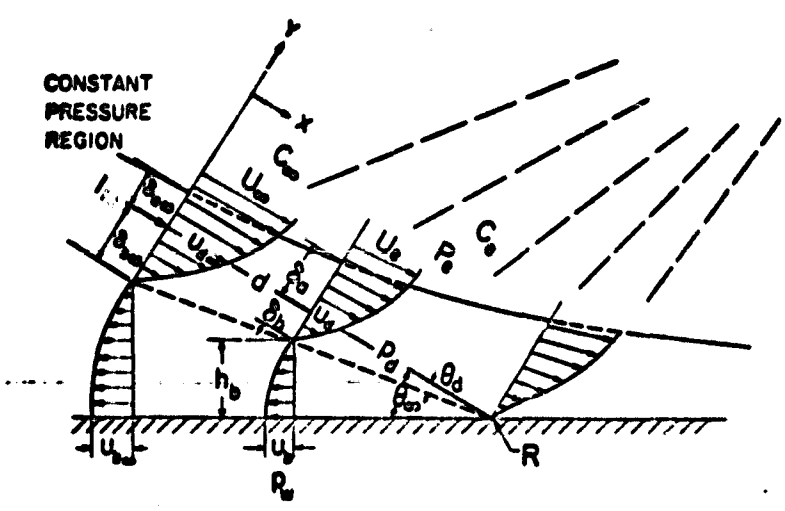

Figure 2 The Flow Model for Recompression Study

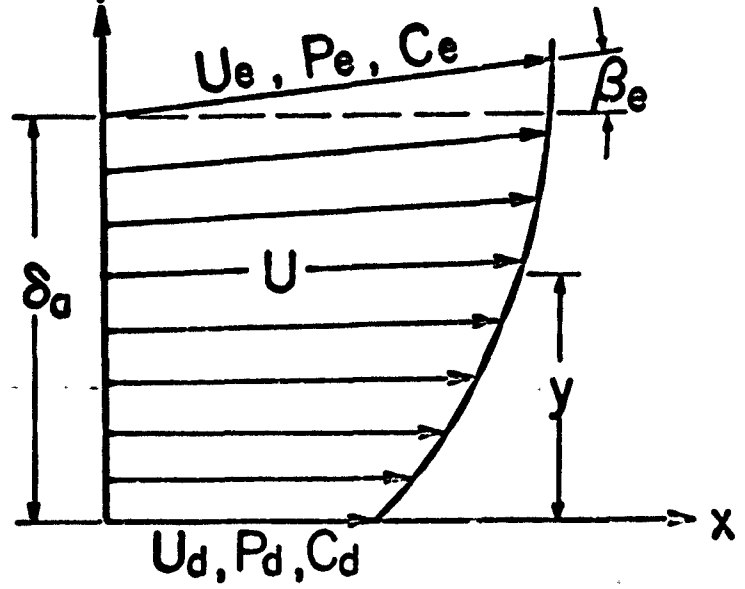

Figure 3a The Upper Viscous Layer

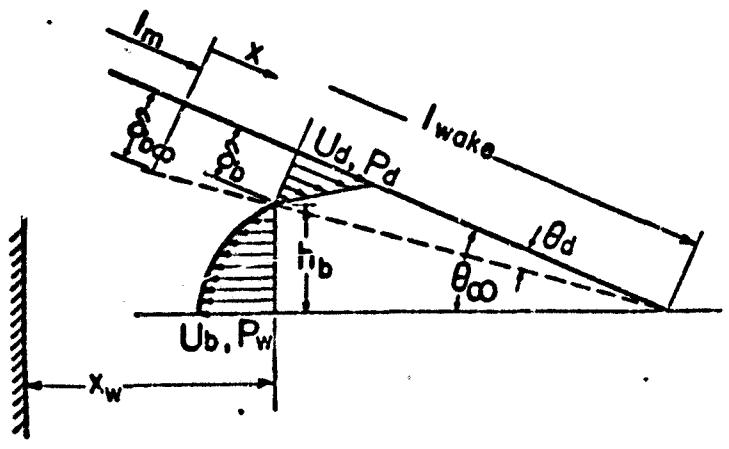

Figure 3b The Lower Viscous Layer

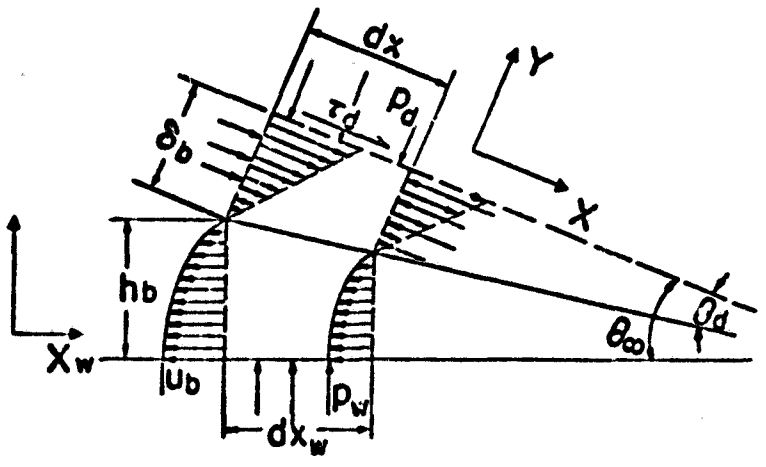

Figure 4a Elementary Control Volume for Lower Viscous Flow Region

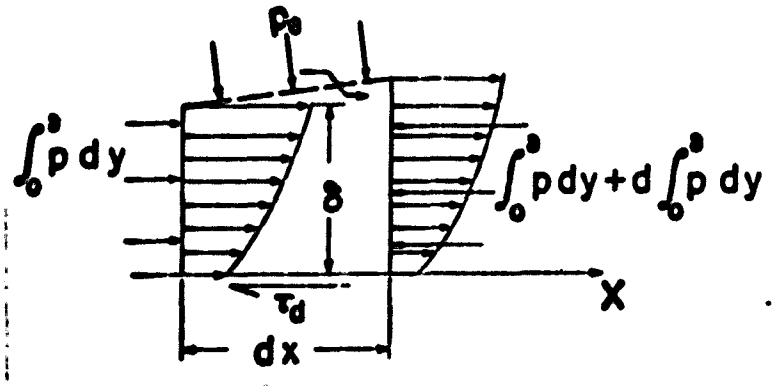

Figure 4b Elementary Control Volume for Upper Viscous Layer

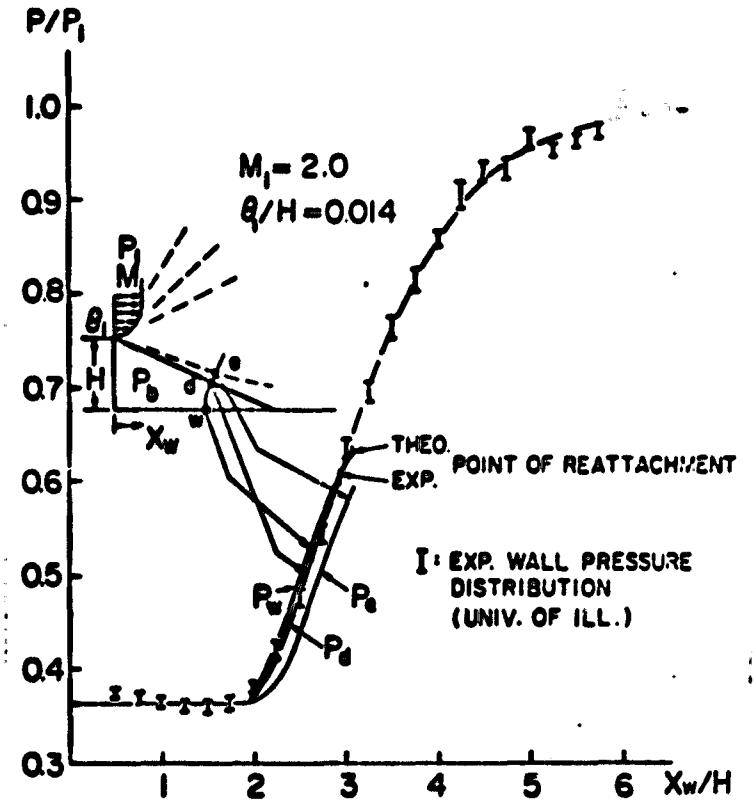

Figure 5 Theoretical and Experimental Wall Pressure Distribution for $M_1 = 2$, $\theta_1/H = 0.01$

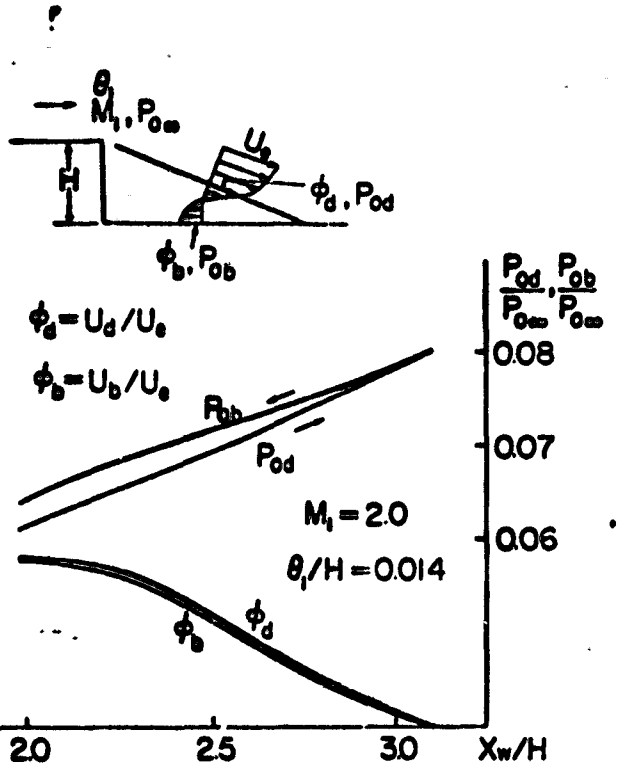

Figure 6 Variation of p_{od}, p_{ob}, ϕ_d, and ϕ_b

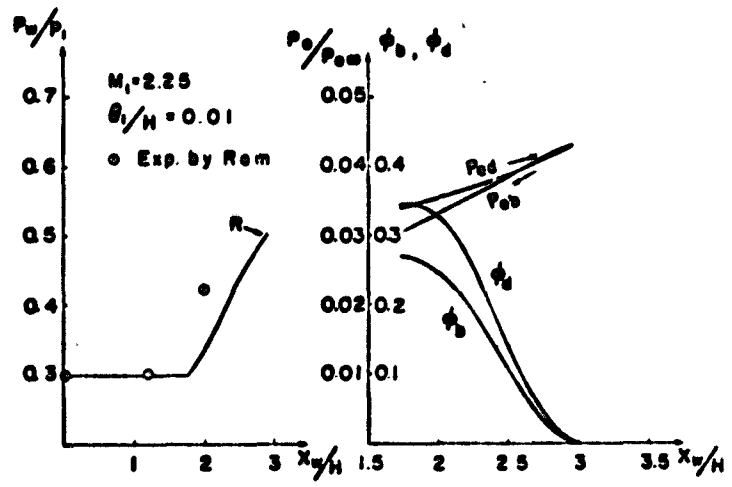

Figure 7 Results for $M = 2.25, \theta_1/H = 0.01$

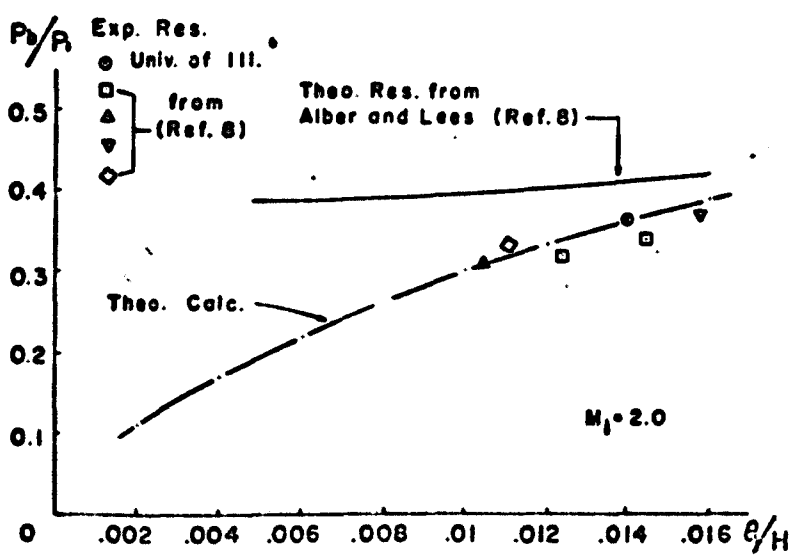

Figure 8 Influence of Initial Momentum Thickness on the Base Pressure Ratio (M = 2.0)

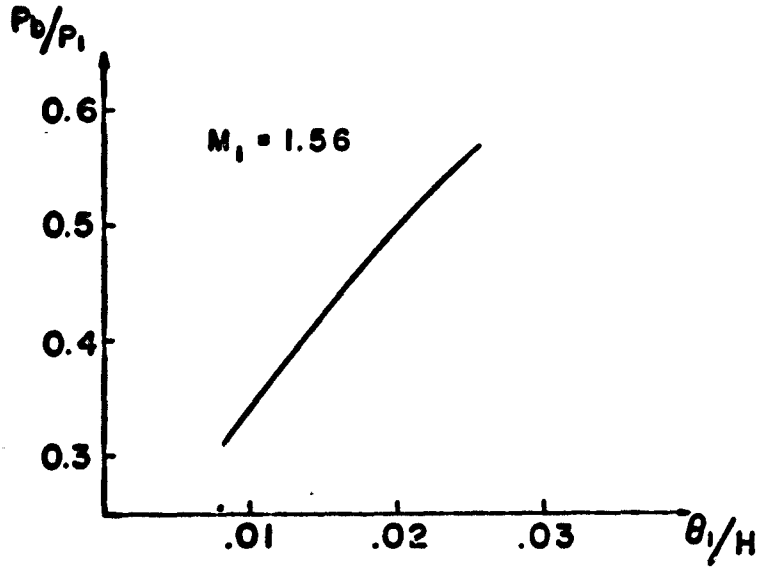

Figure 9 Influence of Initial Momentum Thickness on the Base Pressure ratio (M = 1.56)

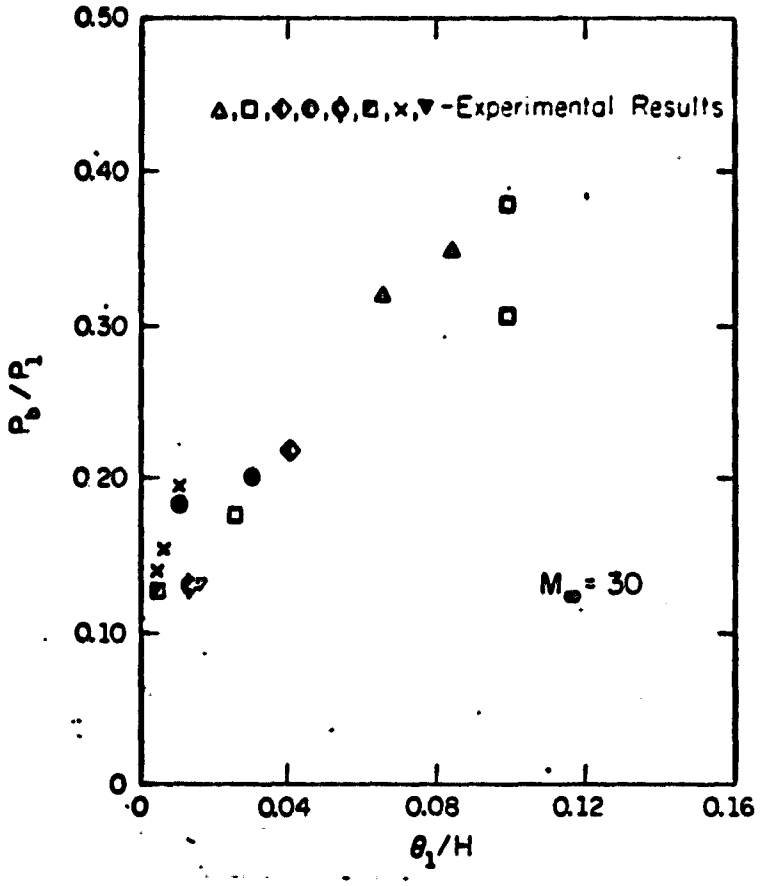

Figure 10 Experimental Base Pressure Ratio for M = 3.0 (Adapted from Ref. 16)

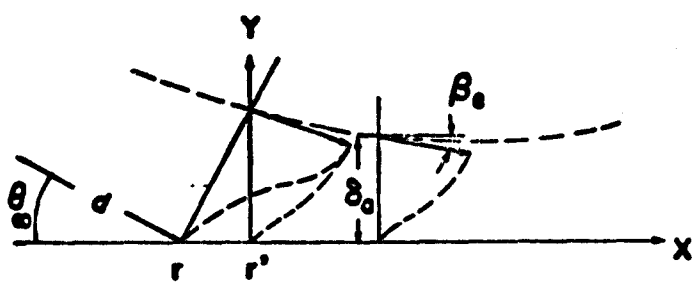

Figure 11 Downstream Flow Field